HHS Public Access

Author manuscript

Biochem Pharmacol. Author manuscript; available in PMC 2019 October 01.

Published in final edited form as:

Biochem Pharmacol. 2018 October ; 156: 135–146. doi:10.1016/j.bcp.2018.08.021.

Ethanol Targets Nucleoredoxin/Dishevelled Interactions and Stimulates Phosphatidylinositol 4-phosphate Production *In vivo* and *In vitro*

Jaime Arellanes-Robledo[1,2,*], **Karina Reyes-Gordillo**[1,*], **Joseph Ibrahim**[1], **Leslie Leckey**[1], **Ruchi Shah**[1], and **M. Raj Lakshman**[1]

[1]Lipid Research Laboratory; VA Medical Center, and Department of Biochemistry and Molecular Medicine, The George Washington University Medical Center. Washington, D.C. USA.

[2]Laboratory of Hepatic Diseases; CONACYT Research Fellow – National Institute of Genomic Medicine (INMEGEN). CDMX, Mexico.

Abstract

Nucleoredoxin (NXN) is a redox-regulating protein potentially targeted by reactive oxygen species (ROS). It regulates molecular pathways that participate in several key cellular processes. However, the role of NXN in the alcohol liver disease (ALD) redox regulation has not been fully understood. Here, we investigated the effects of ethanol and ethanol plus lipopolysaccharide, a two-hit liver injury model (Ethanol/LPS), on NXN/dishevelled (DVL) interaction and on DVL-dependent phosphoinositides production both in mouse liver and in a co-culture system consisting of human hepatic stellate cells (HSC) and ethanol metabolizing-VL17A human hepatocyte cells. Ethanol and two-hit model increased Nxn protein and *mRNA* expression, and 4-hydroxynonenal adducts. Two-hit model promoted Nxn nuclear translocation and Dvl/Phosphatidylinositol 4-kinase type-IIα (Pi4k2a) interaction ratio but surprisingly decreased Dvl protein and *mRNA* levels and reverted ethanol-induced Nxn/Dvl and Dvl/frizzled (Fzd) interaction ratios. Ethanol resulted in a significant increase of Dvl protein and *mRNA* expression, and decreased Nxn/Dvl interaction ratio but promoted the interaction of Dvl with Fzd and Pi4k2a; formation of this complex induced phosphatidylinositol 4-phosphate [PI(4)P] production. Ethanol and LPS treatments provoked similar alterations on NXN/DVL interaction and its downstream effect in HSC/VL17A co-culture system. Interestingly, ROS and glutathione levels as well as most of ethanol-induced alterations were modified by NXN overexpression in the co-culture system. In conclusion, two-hit model of ethanol exposure disrupts NXN/DVL homeostatic status to allow DVL/FZD/PI4K2A complex formation and stimulates PI(4)P production. These results provide a new mechanism showing that

*Corresponding authors: Karina Reyes-Gordillo; Department of Biochemistry, The George Washington University and Lipid Research Laboratory, VA Medical Center, 50 Irving Street, NW, Washington, DC. 20422. Tel: +1 202 745 8330; Fax: +1 202 462 2006. karrygor@gwu.edu. Jaime Arellanes-Robledo; INMEGEN. Periférico Sur No. 4809, Col. Arenal Tepepan, Del. Tlalpan. CDMX. 14610. Tel: +5255 5350 1900; Ext. 1218. jarellanes@inmegen.gob.mx.

Conflict of interest

Authors have no conflict of interest.

NXN also participates in the regulation of phosphoinositides production that is altered by ethanol during alcoholic liver disease progression.

Keywords

Alcoholic liver disease; Nucleoredoxin; Oxidative stress; Phosphoinositide; Redox regulation

1. Introduction

Alcoholic liver disease (ALD) is a complex process involving a spectrum of progressive molecular and morphological alterations starting from steatosis toward steatohepatitis, fibrosis, cirrhosis, and about 15% of patients with established alcoholic cirrhosis develop hepatocellular carcinoma [1]. These alterations are closely linked to the imbalance in cellular redox status since reactive oxygen species (ROS) produced due to chronic ethanol consumption play a key role in pathophysiology of ALD. However, ethanol *per se,* is not solely responsible for ROS production and ALD progression. There are strong experimental evidences showing that ethanol induces leaky gut leading to the release of lipopolysaccharides (LPS), a bacterial-derived endotoxin, into the bloodstream; the released LPS potentiate liver injury initiated by ethanol through an inflammatory-dependent mechanism. This phenomenon has been proposed as a two-hit mechanism of the pathogenesis of ALD; thus, while the first hit is the direct result of ethanol-induced oxidative stress the second hit is by LPS that perpetuate the damage not only in the liver [2–5] but also in others organs such as heart [6]. A number of experimental evidences strongly support the two-hit model of ALD (for details review reference [2]). In normal physiological conditions, the intracellular redox status depends on the balance between pro-oxidants production and endogenous antioxidant activity where the excessive ROS production is generally counteracted by ubiquitously expressed antioxidant molecules such as glutathione, glutaredoxin and thioredoxin (TXN). However, when ROS levels induced by ethanol and LPS exceed the capacity of the endogenous antioxidants, cells are exposed to oxidative stress which causes severe dysfunctions or cell death; therefore, redox balance plays a critical role in the alcohol-mediated cellular fate. It is well known that the main role of antioxidant molecules is to sense and balance the fluctuations of the intracellular ROS levels; however, increasing interest has been paid to their role as redox sensor and intermediary signaling regulator in response to oxidative stress [7].

Nucleoredoxin (NXN), a redox-regulating protein of the TXN family, is a potential target of ROS. Several studies have revealed that NXN regulates different signaling pathways in a redox-dependent manner. NXN is a key player in the redox regulation of the Wingless (WNT)/β-catenin signaling pathway, which is critical in the cell physiology and its dysregulation is related to carcinogenesis [8, 9]. NXN negatively regulates WNT/βcatenin pathway by interacting with Dishevelled (DVL), an essential mediator in the Wnt signaling; however, increased ROS production might dissociate this interaction which enables DVL to activate the downstream WNT/β-catenin signaling pathway [9]. Hayashi et al reported that NXN also negatively mediates Toll-like receptor-4/Myeloid differentiation primary response gene-88 (TLR4/MYD88) signaling pathway by recruiting Flightless-I (FLII) to MYD88 and

regulates the nuclear translocation of NF-κB, a transcription factor that modulates innate immunity and inflammation [10]. Furthermore, NXN also interacts with protein phosphatase-2A (PP2A), an enzyme that participates in DNA replication and cell differentiation processes [11]; with SEC63, a protein that might be involved in protein transport into the endoplasmic reticulum (ER) [12]; and with phosphofructokinase-1 (PFK-1), a glycolytic enzyme that its alteration contributes in multiple human diseases such as cancer [13]. These evidences place NXN redox sensor as the hub of different redox sensitive pathways and thus implicate NXN in the homeostatic functioning of several cellular processes such as immunity, inflammation and cell migration, DNA replication and cell differentiation, protein transport into the ER and glycolysis. Recently, we have shown that acetaldehyde, the first metabolite of ethanol oxidation, mediates β-catenin in a WNT-independent pathway through the imbalance of NXN/DVL interaction ratio that in turn induces β-catenin nuclear translocation and activates fibrogenesis in human hepatic stellate cells (HSC) [14]. If acetaldehyde is able to destabilize NXN/DVL interaction *in vitro*, then it is logical that ethanol-induced oxidative stress *in vivo* leads to the disruption of NXN interactions; however, this phenomenon still remains unexplored. Therefore, we hypothesize that chronic ethanol consumption impairs NXN/DVL interaction ratio and subsequently alters DVL-dependent phosphoinositides (PIs) production during ALD progression. Thus, here we determine the effects of chronic ethanol consumption on the status of NXN interaction with DVL in the mouse liver and in a co-culture system consisting of human HSC and ethanol metabolizing-VL17A hepatocyte-like cells and overexpressing NXN. Our findings show a new mechanism by which, in addition to all cellular processes above described, NXN also participates in the regulation of phosphatidylinositol 4-phosphate [PI(4)P] production, which is altered during the ALD progression.

2. Materials and Methods

2.1. Animals

Animals received proper care in accordance with the Institutional Animal Use and Care Committee of the Veteran Affairs Medical Center and of The George Washington University. Animals were subjected to a chronic ethanol/binge model, a widely used model that includes the high-fat Lieber-DeCarli diet regime plus single-binge of ethanol to induce the early stage of ALD [15]. In the present study, we have further modified it by including an acute treatment with lipopolysaccharide (LPS) because of the fact that chronic ethanol exposure leads to leaky gut resulting in the release of endotoxin to cause further damage to the liver. Thus, after an acclimatization period, six-week-old female wild-type C57BL/6 mice (body wt ~20g) were randomized into control, Ethanol/Binge and Ethanol/Binge/LPS groups (six mice per group). Animals were fed *ad libitum* and housed in a controlled environment with a 12h light/dark cycle. The high-fat Lieber-DeCarli liquid diet was used with a 16 days ramp-up period divided in 2 days per alcohol concentration as follow: control diet (0), 1, 2, 2.5, 3, 3.5, 4 and 4.5%, and then 5% ethanol for 4 weeks to mimic the consequences of ethanol in human alcoholics, in mice liver [16]. Control group (**C**) was pair-fed with a isocaloric diet; Ethanol/Binge group (**E**) was fed with 5% (w/v) ethanol diet for 4 weeks and then it received a single oral dose of 3.2 g ethanol per kg body wt (stock solution of 32% w/v ethanol in saline), as previously reported [4, 15, 17]; Ethanol/Binge/LPS group, simplified as

two-hit model (**TH**) [2–5, 15], was treated similarly as the Ethanol/Binge group, but in addition, each animal also received a single dose of lipopolysaccharides (LPS, 2 mg/kg, i.p. Sigma; St. Louis, MO). Lipopolysaccharides doses were selected according to previous investigations where the acute LPS effects on ALD models were evaluated [2]. Six hours after ethanol and/or LPS administration, each animal was euthanatized by exsanguination under isoflurane anesthesia. Immediately, plasma was separated from the blood and a piece of the dissected liver was split and saved in Trizol reagents (Life Technologies, Grand Island, NY) for mRNA extraction. Other pieces were processed for total, cytosolic and nuclear protein extracts and for confocal microscopy. All collected samples were stored at −75°C for further analyses.

2.2. Cell cultures

Hepatic stellate cells were isolated from human livers obtained during gastric bypass surgery for morbid obesity by the pronase-collagenase method as previously described [14, 18]. Activated HSC were grown to confluence in Dulbecco's modified Eagle's medium F12 (DMEM-F12, from ATCC; Manassas, VA) supplemented with 10% (v/v) fetal bovine serum (FBS, HyClone; Thermo Fisher Scientific. Waltham, MA) and 1% (v/v) penicillin/streptomycin (Sigma; St. Louis, MO). VL17A cells were a courtesy of Dr. Dahn L. Clemens from the Liver Study Unit, VA Medical Center, Omaha; Nebraska. Briefly, VL17A cells are HepG2 cells that constitutively express both cytochrome P450 2E1 (CYP2E1) and alcohol dehydrogenase (ADH) enzymes, were generated as previously described [19]. These cells were grown to confluence in similar culture medium than activated HSC but in addition, it was supplemented with 5 mg/l insulin-transferrin-sodium selenite (ITS, Roche, Branchburg, NJ) and dexamethasone 10^{-7} M (Sigma; St. Louis, MO). Geneticin and Zeocin (400 mg/l; Life Technologies, Grand Island, NY) were added to the culture media as selective antibiotics. Co-cultures of HSC/VL17A cells were cultured in ratio of 1:10 to closely mimic the conditions in whole liver *in vivo* [20]. Co-cultures were grown to semi-confluence in DMEM-F12 supplemented with 10% (v/v) FBS, 1% (v/v) penicillin/streptomycin, 5 mg/l ITS and dexamethasone 10^{-7} M. Eighteen hours before ethanol exposure, culture medium was replaced for DMEM-F12-reduced FBS (0.1%, v/v) medium to synchronize cells activity and then cells were subjected to different treatments indicated below.

2.3. Nucleoredoxin transfection and treatments

Co-cultures were transfected with 1 μg/ml of NXN or empty vector for 24 h using Lipofectamine LTX & Plus Reagent kit in OPTI-MEM medium (Life Technologies; Grand Island, NY) according to the manufacturer instructions; then, OPTI-MEM medium was replaced by DMEM-F12-reduced FBS medium. After 18 h ethanol was added at 100 mM final concentration for 48 h. Then, co-cultures were treated with LPS (1 μg/ml) and incubated for 3 h. To maintain stable ethanol concentration during the incubation time, cell cultures were placed in a plastic container containing 100 mM ethanol in sterile water. Finally, cultures were harvested and protein and RNA were extracted and stored at −75°C for further analyses. In total, five independent NXN transfection experiments were carried out in duplicated. Nucleoredoxin plasmid (A friendly courtesy of Drs. Funato and Miki from the Institute of Medical Science, University of Tokyo, Japan) was cloned using One Shot Top10 chemically competent *E. coli* cells (Life Technologies, Grand Island, NY). The empty

vector was prepared and cloned after excising the NXN cDNA; in our laboratory, the transfection efficiency of NXN vector averaged 85 ± 3%.

2.4. Lipid extraction and phosphatidylinositol 4-phosphate [PI(4)P] quantification

For lipids extraction from mice livers (~50 mg), tissues were homogenized in 0.5 ml of ice-cold PBS buffer supplied with Complete and PhosSTOP (Roche; Branchburg, NJ) as protease and phosphatase inhibitor cocktail, respectively. Lipids extracted from coculture cells were obtained by mixing the cell pellets (~$1.5X10^6$ cells/pellet) with the same buffer used for lipid extraction from mice liver. A 10 μl aliquot was separated for protein quantification. Lipid extraction procedure was carried out as previously described [21, 22]. Lipid extracts were dissolved directly in ethanol at room temperature, loaded into a microplate, and dried under vacuum; then, PI(4)P concentration was determined by enzyme linked immunosorbent assay (ELISA) by using a mouse anti-PI(4)P IgM antibody (ZP004; Echelon Biosciences Inc. Salt Lake City, UT), as previously reported [21]. Negative controls were incubated only with secondary antibody and their optical densities were considered as blank values. Peroxidase activity was detected using TMB peroxidase substrate kit (Vector Labs. Burlingame, CA) and the signal was measured at 650 nm.

2.5. Quantitative PCR analysis

Synthesis of cDNA was performed from 1 μg of total RNA using the M-MLV Reverse Transcriptase (Life Technologies, Grand Island, NY), according to the provider instructions. Real-time quantitative polymerase chain reactions (qPCR) were performed using Power SYBR® PCR Master Mix in a StepOneplus Real Time PCR-System (Life Technologies, Grand Island, NY) and fluorescence was measured in each elongation step. Mice primer sequences for *Nxn* (NM_008750.5) were 5'TGGTGGGAAAATGAATAGCC-3' and 5'-GCTGAATCTTGGGAAGATGG-3'; for *Dvl1* (NM_001356381.1) were 5'-CCTGGGACTACCTCCAGACA-3' and 5'-CATGGTGGAGTCTGTGATGC-3'; for *Dvl2* (NM_007888.3) were 5'CTCATGACCAGTGAGCTGGA-3' and 5'-CTTCTCCATGTTGAGCGTGA-3'; for *Dvl3* (NM_007889.3) were 5'-CGCCTCATGAGAAGACACAA-3' and 5'-ATCACCTCGCTCATTGCTTT-3'; and for *18s* (NM_011296.2) were 5'CAGAAGGATGTGAAGGATGG-3' and 5'-CAGTGGTCTTGGTGTGCTGA-3'. Transcription products were normalized using *18s* as reference gene and quantified by comparative ΔΔCT method as previously described [23].

2.6. Protein extraction

Total protein extracts were prepared as previously reported [14]. Briefly, lysis buffer contained 50 mM Tris (pH 8), 150 mM NaCl, 200 mM EDTA, 100 mM NaF, 10 mM sodium pyrophosphate, 2 mM Na_3VO_4, 1 mM phenylmethylsulfonyl fluoride, 0.5% (v/v) NP-40, (All from Sigma; St. Louis, MO), Complete and PhosSTOP (Roche, Branchburg, NJ). Lysates were incubated on rocking for 30 min, centrifuged at 16000 *g* for 10 min at 4°C and stored at −75°C for further analyses. Cytosolic and nuclear protein from mice liver and co-culture cells were extracted as previously described with some modifications [24]. While frozen hepatic tissues (~100 mg) were first homogenized in 1.0 ml of ice-cold lysis buffer **A**, cells were washed once with ice-cold PBS and then lysed in 0.5 ml of the same buffer **A** (10

mM HEPES, pH 7.9, 10 mM KCl, 0.1 mM EDTA, 0.1 mM EGTA (All from Sigma; St. Louis, MO), Complete and PhoSTOP (Roche, Branchburg, NJ). Lysed samples were incubated on ice for 15 min with occasional mixing. Then, 30 μl of 10% NP-40 solution was added; vortexed vigorously for 15 sec, centrifuged for 30 sec at 16000 *g* and supernatant was stored at −75°C as the cytosolic protein fraction. Pellets containing intact nuclei were washed twice in buffer **A**, resuspended in ice-cold buffer **B** [20 mM HEPES, pH 7.9, 0.4 mM NaCl, 1 mM EDTA, 1 mM EGTA, 0.6% NP-40 (All from Sigma; St. Louis, MO), Complete and PhoSTOP (Roche, Branchburg, NJ)], rocked in a shaking platform for 15 min at 4°C, centrifuged in a microcentrifuge for 30 min at 16,000 *g* and supernatant was stored at −75°C as the nuclear protein fraction for further analyses. All procedures were performed at 4°C to reduce protein degradation.

2.7. Western blot analysis

Equivalent amounts of boiled protein in Laemmli's buffer were analyzed through SDSPAGE and transferred to a PVDF membrane. Antibodies against NXN (GTX107039) and ADH1 (GTX62515) were purchased from GeneTex Inc (Irvine, CA); CYP2E1 (ab28146) was purchased from Abcam (Cambridge, MA); DVL (goat-G19 and mouse-B4), DVL1 (3F12), DVL2 (H75), DVL3 (4D3), PI4K2A (H40), FZD (H300), Lamin B (M20), and 4hydroxynonenal (4-HNE; P16) were purchased from Santa Cruz Biotechnology (Santa Cruz, CA); and β-actin (A5441) and Vinculin (V9131) were purchased from Sigma (St. Louis, MO). Protein loading was confirmed by reprobing the blots with anti-β-actin or anti-Lamin B for cytosolic and nuclear fractions, respectively. Densitometric analyses were carried out using ImageJ software (NIH).

2.8. Immunofluorescence staining

Co-cultures plated in two well chamber slides were rinsed twice in ice-cold PBS, fixed with 4% formaldehyde in PBS (pH 7.4) for 10 min at room temperature, washed three times and incubated for 1 h with washing solution [0.25% Triton X-100 in PBS (PBST)]. Then, co-cultures were blocked with 1% BSA in PBST for 30 min at room temperature and mouse anti-Vinculin (1:400) and rabbit anti-CYP2E1 (1:1000) were incubated overnight at 4°C in blocking solution. After washing, co-cultures were incubated for 1 h at room temperature in the dark either with Alexa Fluor 488 donkey anti-mouse 1:500 or with Alexa Fluor 568 donkey anti-rabbit 1:500 (Life technologies, Grand Island, NY) for Vinculin and CYP2E1 detection, respectively. Nuclear DNA was stained with ToPro 1:500 (Life Technologies, Grand Island, NY) for 30 min at room temperature, respectively. Finally, co-cultures were rinsed, drained and fixed using Prolong Gold antifade reagent (Life Technologies, Grand Island, NY). Pictures were captured using Zeiss LSM 710 Axio Observer confocal microscopy.

2.9. Reactive oxygen species and glutathione determination

Reactive oxygen species (ROS) were determined in black 96-well microplates by labeling approximately 7×10^3 cells/well with 25 μM of 2',7'-dichoroflurescein diacetate (DCFDA) for 30 min at 37°C in the dark; then, co-cultures were treated with ethanol for 48 hours followed by LPS for 3 h. Fluorescence intensity was measured at 535 nm (excitation at 485

nm). Glutathione (GSH) content was determined after alcohol and/or LPS treatments according to the GSH assay kit instructions (CS0260, Sigma, St. Louis, MO) [25].

2.10. Immunoprecipitation (IP) assay

Total protein from liver tissues and cell co-cultures were processed in the ice-cold lysis buffer containing 20 mM Tris-Cl, pH 7.8, 137 mM NaCl, 1% (v/v) Nonidet P40, 10% (v/v) glycerol, 2 mM EDTA (All from Sigma; St. Louis, MO), supplied with Complete and PhoSTOP (Roche, Branchburg, NJ) as previously described [14]. Proteins of interest were immunoprecitated with protein A/G Plus-Agarose complex beads (sc2003, Santa Cruz Biotechnology, Santa Cruz, CA) and either mouse anti-Dvl or mouse anti-DVL3 for mice and co-culture samples, respectively. Co-precipitated were normalized by reprobing the blots to detect the constant regions (heavy chains) of the immunoglobulins used for IP assay [26].

2.11. Statistical analyses

Statistical analyses were performed using GraphPad Prism 7.0 software. Data calculations were performed using either one-way ANOVA followed by Bonferroni's posthoc test for multiple comparison or Student *t*-test when only two groups were compared. All experiments were performed at least in triplicate. Data are expressed as mean ± S.E.M. Differences were considered significant when $p<0.05$.

3. Results

3.1. Ethanol chronic consumption alters Nxn and Dvl status in mice liver

We explored the effects of Ethanol/Binge (E) as well as Ethanol/binge/LPS (TH) model on Nxn status. Both models significantly increased more than 2.0 ($p<0.001$) and 2 ($p=0.02$) fold *Nxn* mRNA expression and 1.6 ($p=0.004$) and 1.5 ($p=0.007$) total protein levels, respectively, compared to the controls (Figs. 1A-B). Ethanol/Binge and Ethanol/Binge/LPS showed a differential effect on Nxn protein compartmentalization. While increased Nxn protein levels were retained in the cytosol by Ethanol/Binge (1.5 fold, $p=0.03$), Ethanol/Binge/LPS model reduced it by 33% ($p=0.03$). In contrast, Ethanol/Binge/LPS induced the nuclear translocation of Nxn by 1.5 ($p=0.03$) fold (Figs. 1C-D). When we also investigated the effects of these models on Dvl status, we found that Dvl protein levels were increased more than 1.6 ($p=0.02$) fold by Ethanol/Binge, but this increment was abolished 50% ($p=0.03$) by Ethanol/Binge/LPS model compared to the controls (Fig. 2A). Once we found that ethanol altered total Dvl protein levels, we then determined the involvement of the Dvl homologs (Dvl1, Dvl2 and Dvl3) in this process [27]. We found that *Dvl1* and *Dvl2* mRNA expression were not significantly affected by either model; however, *Dvl3* was increased 1.2 ($p=0.008$) fold by Ethanol/Binge but decreased 34% ($p=0.02$) by Ethanol/Binge/LPS model compared to the controls (Fig. 2B). At protein level, Dvl1 was not detected in the liver samples and Dvl2 was diminished by 58% ($p=0.02$) by Ethanol/Binge/LPS model, while Dvl3 levels were induced 2.5 ($p=0.01$) fold by Ethanol/Binge, but this increment was diminished at controls levels by Ethanol/Binge/LPS model effect (Fig. 2C).

3.2. Disruption of Nxn/Dvl interaction by ethanol promotes PI(4)P production *in vivo*

To determine the oxidative ethanol effects on the redox sensitive Nxn/Dvl interaction, we first evaluated the levels of 4-HNE protein adducts. As expected, formation of 4-HNE was increased 1.8 (p=0.005) fold by Ethanol/Binge and Ethanol/Binge/LPS models compared to controls (Fig. 3A). Immunoprecipitation analysis revealed that Nxn, Fzd and Pi4k2a proteins were efficiently coimmumoprecipitated by an anti-Dvl antibody and confirmed Dvl induction by Ethanol/Binge (Figs. 2A and3A). Ethanol/Binge decreased the Nxn/Dvl complex binding ratio by 54% (p=0.001); unexpectedly, Ethanol/Binge/LPS model partially restored this ratio. In contrast, Fzd/Dvl complex binding ratio was significantly increased more than 1.5 (p=0.004) fold by Ethanol/Binge, but this increment was reverted to control levels by the Ethanol/Binge/LPS model. Both models also increased Pi4k2a levels more than 1.4 (p=0.008) fold compared to the controls, (Fig. 3B). Additionally, since production of PI(4)P depends on Dvl/Fzd/Pi4k2a complex formation [21], we then performed ELISA analyses in order to investigate the ethanol effect on PI(4)P production. Interestingly, we found that both models stimulated more than 1.7 (p<0.005) fold the production of PI(4)P compared to the controls (Fig. 3C).

3.3. Ethanol effect on NXN-dependent regulation in an *in vitro* model

First, by immunofluorescence analyses we determined the expression of vinculin, a HSC marker [28], and that of CYP2E1 to confirm its induction by ethanol in VL17A cells. As shown in Fig. 4A, vinculin was detected in both HSC and VL17A cells; however, CYP2E1 overexpression was stimulated by ethanol only in VL17A cells. After NXN transfection in the co-culture system, we determined the transfection efficiency (Fig. 4B). Then, to discard a possible adverse effect of NXN transfection on VL17A cells overexpressing CYP2E1 and ADH1, we determined their protein levels in co-cultures treated with ethanol and/or LPS to mimic the Ethanol/Binge and Ethanol/Binge/LPS models in our *in vitro* system. As shown in Fig. 4C, NXN transfection did not affect the induction of both CYP2E1 and ADH1 by ethanol exposure. Neither CYP2A1 nor ADH1 basal protein levels were affected by NXN transfection. Ethanol induced CYP2E1 by at least 6 fold and more than 2 fold change in ADH1 protein levels (p<0.001). Nucleoredoxin protein levels were induced 1.6 (p=0.003) and 1.4 (p<0.001) fold change by ethanol in untransfected and NXN-transfected cells, respectively, compared to their respective controls. Conversely, LPS alone or in combination with ethanol partially interfered on NXN expression induced by ethanol.

Then we evaluated both cytosolic and nuclear NXN compartmentalization after ethanol and/or LPS treatments. Fig. 5A shows that NXN levels increased more than 6 and 1.4 fold change (p<0.001) by ethanol effect in cytosolic fraction of NXN-transfected cells compared to untransfected and NXN-transfected controls, respectively. Neither ethanol nor LPS modified the cytosolic location of NXN in untransfected cells. Ethanol induced NXN nuclear translocation by 1.2 fold change (p=0.005) in NXN-transfected cells compared to NXN-transfected controls (Fig. 5B). Although there was an increment tendency induced by ethanol alone or in combination with LPS in untransfected cells, they were not significant. As evaluated in *in vivo* model, we then determined the effects of ethanol and/or LPS on DVL variant proteins. While DVL1 was undetected, DVL2 and DVL3 levels were clearly

observed but DVL3 signal was stronger than DVL2. Neither ethanol nor LPS significant modified their expression levels (Fig. 5C).

To determine the effects of ethanol and LPS on oxidative stress parameters, we then evaluated ROS and GSH levels in the co-culture system. We found that ethanol either alone or in combination with LPS significantly induced ROS levels (ethanol 1.4; LPS 1.3; and ethanol plus LPS 1.5 fold change compared to controls, $p<0.001$) in untransfected cells (Fig. 6A). Interestingly, neither ethanol nor LPS alone or in combination induced ROS levels higher than NXN-transfected controls. On the other hand, both ethanol and LPS alone or their combination induced at least 1.6 ($p<0.001$) fold change the levels of GHS in untransfected cells compared to controls (Fig. 6B). Even though ethanol or/and LPS significantly ($p<0.01$) induced GSH levels in NXN-transfected cells compared to NXN-transfected controls, these inductions were 26, 30 and 13% ($p<0.001$) less than those induced in untransfected cells compared to the same treatments.

3.4. NXN overexpression prevents NXN/DVL complex disruption and PI(4)P production induced by both ethanol and LPS in HCS/VL17A co-culture

To explore whether ethanol and/or LPS have similar oxidative injury effects *in vitro* than in mice liver, we investigated the effects of those reagents on DVL/NXN complex and in PI(4)P production in the co-culture system. In our previous results, we showed that from DVL variant proteins, DVL3 was the strongest variant expressed in the co-culture system (Fig. 5C). Based on that, we immunoprecipitated DVL3 and determined its binding complex status with NXN, FZD and PI4K2A. As expected, in NXN-transfected cells NXN protein was co-precipitated more than 1.5 fold change ($p<0.001$) compared to untransfected controls (Figs. 7A-B). NXN/DVL3 binding complex was disrupted by 15 ($p=0.002$), 21 ($p=0.03$) and 15% ($p=0.04$) in ethanol, LPS and their combination, respectively, compared to the same treatment in untransfected cells. In NXN-transfected cells, LPS alone or in combination with ethanol significantly increased NXN coprecipitation by 1.2 fold change ($p<0.001$) and the ratio of NXN/DVL3 binding complex was 20% higher compared to NXN-transfected control cells. Ethanol, LPS and their combination significantly ($p=0.03$) increased DVL3/FZD complex ratio compared to untransfected controls. However, in NXN-transfected cells this ratio decreased 32, 40 and 50% ($p<0.001$) by ethanol LPS and their combination, respectively, compared to NXN-transfected and untransfected controls (Fig. 7A,C). The ratio of DVL3/PI4K2A binding complex was increased 2.1 ($p=0.02$) and 2.3 ($p=0.007$) fold change by ethanol and ethanol plus LPS, respectively, in untransfected cells compared to controls. In NXNtransfected cells ethanol and LPS also increased 2.1 ($p=0.01$) and 2.1 ($p=0.02$) fold change this binding ratio; interestingly, combination of ethanol plus LPS disrupted the DVL3/PI4K2A binding ratio (Fig. 7A,D). Similar than in total protein analysis (see Fig. 5C), DVL3 level by immunoprecipitation analysis was not significantly changed although combination of LPS with ethanol trended to decrease it in untransfected cells (Fig. 7A,E). Finally, to investigate whether the alteration of DVL/FZD/PI4K2A complex modified the production of PI(4)P, we measured it by ELISA in the co-culture system. We found that only ethanol increased 1.5 fold change PI(4)P production ($p=0.01$) in untransfected cells compared to controls. Interestingly, in NXN-transfected cells PI(4)P production was not induced by any reagent but instead, ethanol in combination with LPS

decreased its level 53% (p=0.002) compared to untransfected control cells, and 47% (p=0.03) compared to NXN-transfected controls. All treatments in NXN-transfected cells, significantly decreased PI(4)P production compared to the same treatment in untransfected cells (Fig. 7F).

4. Discussion

Multiple evidences support the causative involvement of oxidative stress produced by the chronic ethanol consumption in the ALD progression. Ethanol has the ability to produce high levels of ROS, deplete endogenous antioxidants and increase oxidative injury biomarkers [29]. In this investigation we used both *in vivo* and *in vitro* models to explore the oxidative stress effects of ethanol on NXN/DVL redox-sensitive interaction. Recently, we have shown that acetaldehyde-induced fibrogenesis is associated to the imbalance of NXN/DVL interaction ratio [14]. With this evidence, we proposed that chronic ethanol consumption could be targeting NXN/DVL redox-sensitive interaction. Both ethanol and two-hit model increased Nxn protein and mRNA levels, and 4-HNE adducts production; and two-hit model but not ethanol alone provoked Nxn nuclear translocation (Fig. 1 & 3). Conversely, ethanol alone induced NXN nuclear translocation in transfected cells (Fig. 5). This NXN behavior was first described when this gene was cloned and its protein product was mainly localized into the nucleus of NXNoverexpressing cultured cells [30]. In both untransfected and transfected cells, ethanol but not LPS alone or in combination with ethanol induced NXN protein levels; this increment was accompanied with increased ROS and GSH levels in untransfected cells but these two parameters were also induced by LPS (Fig. 4 & 6). Contrary to ROS, GSH levels were increased even in NXN-transfected cells but this increment was less than the same treatment of untransfected cells. Considering 4-HNE and ROS as prooxidative and GSH as anti-oxidative parameters, our present findings confirm the potential of ethanol to imbalance the redox status in the liver, implying that ethanol and two-hit model have differential effects on Nxn compartmentalization in liver cells, and reveal that NXN overexpression reduces the oxidative stress promoted by ethanol *in vitro*.

Upon WNT signaling activation, DVL plays a key role to activate β-catenin nuclear translocation by disassembling its destruction complex [27]. By treating cell cultures with H_2O_2 and acetaldehyde, it has been shown that NXN regulates the recruitment of DVL to FZD/low density lipoprotein receptor-related protein-6 (LRP6) complex in a redox-dependent mechanism [9, 14, 27]. Dishevelled has three well-characterized murine isoforms (Dvl1, Dvl2 and Dvl3), broadly expressed in both embryonic development and adult tissues [27]. Our *in vivo* results show that in spite of the fact that all three *Dvl mRNAs* isoforms were expressed in the mice liver, only *Dvl3* expression was significantly induced by ethanol. This result was confirmed at protein level also showing a differential expression in response to ethanol or LPS exposure (Fig. 2). Thus, our results demonstrate that each Dvl isoform may operate in a unique way to various stimuli although they all may work as a network [31].

It is well-known that Wnt signaling pathway might participate in the regulation of different cellular processes of cell proliferation and metabolism including lipid metabolism, among

others [32, 33]. In this regard, the formation of some PI, the phosphorylated product of a class of lipids called phosphatidylinositol, is regulated through Dvl participation. Recently, it was reported that Fzd/Dvl interaction can stimulate the formation of phosphatidylinositol 4,5-bisphosphate [$PI(4,5)P_2$] by sequential actions of PI-4-kinase type II (PI4K2a) and PI-4-phosphate 5-kinase type I (PIP5KI). In this process Dvl directly interacts with the activated form of PI4K2a; thus, all these proteins form a complex upon Wnt3a stimulation and the resultant $PI(4,5)P_2$ is required for Wnt3a-induced clustering and phosphorylation of LRP6 [34]. Subsequent analyzes by the same group showed that production of PI(4)P also dependents on Fzd/Dvl/PI4K2a/PIP5KI complex formation and allows the efficient production of $PI(4,5)P_2$ [21]. Herein we investigated the effects of ethanol and LPS on the status of NXN/DVL interaction and the resultant FZD/DVL/PI4K2A complex formation both *in vivo* and *in vitro*. Our results clearly show that ethanol decreased Nxn/Dvl interaction ratio and as expected, it stimulated the interaction of Dvl with Fzd and its subsequent binding to Pi4k2a *in vivo* (Fig. 3). Similar effects were observed *in vitro* since ethanol and LPS treatments also disrupted NXN/DVL interaction while ethanol preferentially stimulated FZD/DVL/PI4K2A complex formation. Interestingly, NXN overexpression prevented the complex formation by sequestering DVL and impeding its binding to FZD and PI4K2A proteins (Fig. 7). Parallel to this molecular mechanism we also determined whether the modification of NXN/DVL interaction ratio and its downstream effects were in response to the elevated levels of oxidative stress produced by ethanol and/or LPS. Accordingly, 4-HNE (Fig. 3), ROS and GSH (Fig. 6) levels were elevated by ethanol and/or LPS *in vivo* and *in vitro* models, respectively. Again, these inductions were suppressed in NXN overexpressed cells (Fig. 6). An intriguingly result that we obtained was the fact that the disrupted Nxn/Dvl interaction ratio and Fzd/Dvl/Pi4k2a complex formation stimulated by ethanol were surprisingly reverted by two-hit model; a model that mimics the effects of an acute endotoxemia observed in ALD [35]. It is well-known that toll-like receptors (TLRs) facilitate innate immune responses for the initial host defense against endotoxins released by microorganisms [36]. Intestinal microflora are the source of circulating endotoxins such as LPS, and the gut barrier dysfunction leading to elevated intestinal permeability is considered the main cause of endotoxemia in ALD [35]. Although the liver is constantly exposed to LPS from the intestinal microflora, inflammation is not apparent in the healthy liver because of an immunological adaptation process called hepatic tolerance [37]. Recently, it has been shown that low doses of LPS pretreatment attenuated the liver injuries induced by diethylnitrosamine via TLR4 participation in mice and this phenomenon was associated to hepatic tolerance [38]. Additionally, upon LPS stimulation, LPS binds to TLR4 and induces both the recruitment of MYD88 to TLR4 to regulate inflammation by the activation of NF-κB transcription factor and, the interaction of FLII with MYD88 through NXN to avoid the undesirable activation [10]. Together, these supporting data allow us to propose that the interference/reversal of ethanol effects by two-hit model might be first, because of the development of hepatic tolerance with a single LPS administration that might be broken after chronic endotoxin exposure [39]; secondly, it is plausible that after LPS administration, NXN is required to regulate additional molecular events such as the acute activation of TLR4/MYD88-dependent function; for this end, NXN initiates a prioritization of the molecular events to regulate. Because LPS administration aims to enhance subsequent toxic effects induced by ethanol and to mimic the acute

endotoxemia effects in ALD, NXN increases its signalingregulating activity and prioritizes its interaction with DVL and with FLII and MYD88 in order to avoid the hyperactivation of DVL-dependent signaling and TLR4/MYD88 pathway. Further studies are required to understand these mechanisms. Our present concept is supported by the fact that two-hit model also induced NXN expression and nuclear translocation as a mechanism to protect the nuclei from the acute injuries boosted by LPS in the liver microenvironment (Fig. 1). In contrast, the interference of ethanol acute administration on LPS-induced inflammatory response has already been demonstrated [40]. Ethanol inhibits TLRs signaling when a potent LPS dose was provided during ethanol acute intoxication. Thus, our results suggest that ethanol redistributes TLR4 and reorganizes the actin cytoskeleton, thereby impairing the receptor clustering. This effect blunts the full activation of TLR4-mediated downstream signaling, such as NF-κB pathways involved in the inflammatory response [40]. Collectively, these evidences indicate that while ethanol disrupts NXN/DVL homeostatic status to allow FZD/DVL/PI4K2A complex formation, an event initiated by ethanolinduced oxidative stress, two-hit model partially interferes on ethanol effects allowing NXN to move where it is preferentially required and avoid more severe liver alterations; thus, NXN might be acting as a part of TLR4-dependent molecular pool to aid the initial defense against oxidative stress. Accordingly, the overexpression of NXN decreases oxidative stress parameters by functioning as ROS scavengers cooperatively with endogenous GSH in the co-culture microenvironment. The fact that GSH and ROS levels were diminished in NXN-overexpressing cells exposed to stressor reagents supports this concept (Fig. 6).

Phosphoinositides have key regulatory roles in cell physiology including signal transduction, regulation of membrane trafficking, migration, among others [41, 42]. There are evidences showing that a number of infectious agents hijack the PIs regulatory systems of host cells for their intracellular movements, replication, and assembly [41]. Here, we investigated whether PIs are targeted by chronic ethanol consumption through determining its effect on FZD/DVL/PI4K2A complex formation and the subsequent PI(4)P production. Although two-hit model reversed the complex formation we found that not only ethanol but also two-hit model increased PI(4)P production. Even though several evidences have shown that altered expression and/or activity of enzymes that regulate PIs metabolism such as phosphoinositide 3-kinase (PI3K)/phosphatase and tensin homolog (PTEN), are linked to the development of several hepatic diseases [43]; to our knowledge, there is no evidence showing the direct participation of PIs in ALD. Our results show that PI(4)P, a precursor of $PI(4,5)P_2$, was increased by ethanol and two-hit model *in vivo* and by ethanol *in vitro*, predominantly through the participation of NXN since its overexpression *in vitro* abolished this effect (Fig. 3 & 7). These results also suggest that PI(4)P induced by chronic ethanol consumption might sensitize and facilitate the viral entrance into the liver of chronic alcoholics [41], since it is well-known that the endocytosis of several pathogens such as hepatitis C virus uses the same routes by which cell surface proteins enter the endocytic pathways and hence, rely upon a PI that depends on PI(4)P, $PI(4,5)P_2$ [44]. Thus, the increment of PIs by chronic ethanol consumption might greatly impact on the ALD progression because of its role on the cell physiology and on the sensitization of the liver tissue towards viral infections. To proof this concept further investigations are needed. When there is a low blood ethanol concentration, it is primarily metabolized in the liver by the low

Km alcohol dehydrogenase (ADH) enzyme [45]. However, at excessive ethanol levels, its metabolism is catalyzed by the high Km enzyme CYP2E1. Both enzymes are mainly expressed in the hepatocytes [46]. Although, primary hepatocyte cultures are an excellent system for acute ethanol studies, they eventually lose their ability to metabolize ethanol because of a significant expression decline of these enzymes [19]. VL17A cells express stable catalytically active CYP2E1 and ADH1, and thereby exhibit an enzymatic phenotype similar to hepatocytes in alcoholics [19]. Even though HSC express low levels of ADH, they do not express CYP2E1 [47]; thus, cocultures of VL17A cells and HSC represent a promising model to describe ALD-associated redox alterations since ethanol metabolism by VL17A cells leading to oxidative stress, which in turn activates HSC to boost the oxidative damage in the liver [48]. The usefulness of co-cultures is supported by the fact that the well-functioning of the liver is orchestrated by close interaction among different kinds of liver cells. Thus, the elucidation of true correlation of molecular events among various types of liver cells operating in the whole organ *in vivo* cannot be unraveled by studies involving only one type of liver cells in culture. Therefore, co-cultures including two cell types represent a closer link with *in vivo* models. In this regards, hepatic co-culture systems have already been used for different investigation purposes. For example, co-culture including primary HSC and Kupffer cells show the importance of immune cells in the regulation of fibrogenesis [49]; co-culture including HSC and endothelial cells demonstrate the role of HSC in angiogenesis [50]; co-culture including hepatocytes and HSC show that cell-tocell proximity enhances the initiation of fibrogenesis stimulated by fatty accumulation [51] and more recently; co-culture including endothelial cells and HepG2 cells demonstrate hepatic tissue engineering [52]. Here, we used a human co-culture system consisting of primary HSC and VL17A cells to investigate the role of oxidative stress generated by ethanol metabolism on a redox-regulated molecular mechanism. This coculture system expresses ADH and CYP2E1 enzymes, whose expressions are almost nonexistent in primary hepatocyte cultures; thus, VL17A cells exhibit an enzymatic phenotype similar to normal human hepatocytes. Additionally, HSC represent a hepatic element that provides a closer link with *in vivo* situations where ethanol effects are explored. Based on our results, this co-culture system is viable to complement studies from ALD *in vivo*. Although the co-culture is bearing two stable transfected plasmids; it is still transfectable to be maintained for prolonged periods and therefore we suggest it might be useful for the study of others molecular phenomena related to ALD.

In summary, we describe a mechanism by which ethanol disrupts NXN/DVL homeostatic status and induces FZD/DVL/PI4K2A complex formation to allow PI(4)P production (Fig. 8). These results provide a new mechanism showing that NXN also participates in the regulation of PI production altered by ethanol during ALD progression. We also demonstrate that ethanol and LPS treatments similarly disrupt NXN/DVL interaction ratio and differentially stimulate FZD/DVL/PI4K2A complex formation interactions. These alterations were modified by NXN overexpression in the co-culture system including ROS levels. Finally, based on our present findings and on the broad spectrum of molecular processes that NXN is involved in, we propose that NXN might be a master redox regulator in the cell physiology.

Acknowledgments

This work was funded by the National Institute on Alcohol Abuse and Alcoholism grant RO1 AA010541 (M.R.L). J.A.R. expresses his sincere thanks to CONACYT-Mexico for awarding the fellowships No. 128405 and 151478 as well as to Cátedras-CONACYT program. Authors express their gratitude to Dr. Dahn L. Clemens for providing VL17A cells (Liver Study Unit, VA Medical Center, Omaha; Nebraska) and Drs. Funato and Miki (Institute of Medical Science, University of Tokyo, Japan) for providing NXN plasmid.

Abbreviations

4-HNE	4-hydroxynonenal
ALD	alcoholic liver disease
C	Control group
DCFDA	2',7'-dichoroflurescein diacetate
E	Ethanol/Binge model
ELISA	enzyme linked immunosorbent assay
ER	endoplasmic reticulum
HSC	hepatic stellate cells
LPS	lipopolysaccharide
ROS	reactive oxygen species
PIs	Phosphoinositides
TH	Ethanol/Binge/LPS "two-hit" model

References

[1]. Sid B, Verrax J, Calderon PB, Role of oxidative stress in the pathogenesis of alcohol-induced liver disease, Free radical research 47(11) 894–904. [PubMed: 23800214]

[2]. Schaffert CS, Duryee MJ, Hunter CD, Hamilton BC, 3rd, DeVeney AL, Huerter MM, Klassen LW, Thiele GM, Alcohol metabolites and lipopolysaccharide: roles in the development and/or progression of alcoholic liver disease, World J Gastroenterol 15(10) (2009) 1209–18. [PubMed: 19291821]

[3]. Koteish A, Yang S, Lin H, Huang X, Diehl AM, Chronic ethanol exposure potentiates lipopolysaccharide liver injury despite inhibiting Jun N-terminal kinase and caspase 3 activation, The Journal of biological chemistry 277(15) (2002) 13037–44. [PubMed: 11812769]

[4]. Gustot T, Lemmers A, Moreno C, Nagy N, Quertinmont E, Nicaise C, Franchimont D, Louis H, Deviere J, Le Moine O, Differential liver sensitization to toll-like receptor pathways in mice with alcoholic fatty liver, Hepatology (Baltimore, Md 43(5) (2006) 989–1000.

[5]. von Montfort C, Beier JI, Guo L, Kaiser JP, Arteel GE, Contribution of the sympathetic hormone epinephrine to the sensitizing effect of ethanol on LPS-induced liver damage in mice, American journal of physiology 294(5) (2008) G1227–34. [PubMed: 18325983]

[6]. El-Mas MM, Fan M, Abdel-Rahman AA, Endotoxemia-mediated induction of cardiac inducible nitric-oxide synthase expression accounts for the hypotensive effect of ethanol in female rats, J Pharmacol Exp Ther 324(1) (2008) 368–75. [PubMed: 17925480]

[7]. Fujino G, Noguchi T, Takeda K, Ichijo H, Thioredoxin and protein kinases in redox signaling, Seminars in cancer biology 16(6) (2006) 427–35. [PubMed: 17081769]

[8]. Funato Y, Miki H, Nucleoredoxin, a novel thioredoxin family member involved in cell growth and differentiation, Antioxidants & redox signaling 9(8) (2007) 1035–57. [PubMed: 17567240]

[9]. Funato Y, Michiue T, Asashima M, Miki H, The thioredoxin-related redox-regulating protein nucleoredoxin inhibits Wnt-beta-catenin signalling through dishevelled, Nature cell biology 8(5) (2006) 501–8. [PubMed: 16604061]

[10]. Hayashi T, Funato Y, Terabayashi T, Morinaka A, Sakamoto R, Ichise H, Fukuda H, Yoshida N, Miki H, Nucleoredoxin negatively regulates Toll-like receptor 4 signaling via recruitment of flightless-I to myeloid differentiation primary response gene (88), The Journal of biological chemistry 285(24) (2010) 18586–93. [PubMed: 20400501]

[11]. Lechward K, Sugajska E, de Baere I, Goris J, Hemmings BA, Zolnierowicz S, Interaction of nucleoredoxin with protein phosphatase 2A, FEBS letters 580(15) (2006) 3631–7. [PubMed: 16764867]

[12]. Muller L, Funato Y, Miki H, Zimmermann R, An interaction between human Sec63 and nucleoredoxin may provide the missing link between the SEC63 gene and polycystic liver disease, FEBS letters 585(4) 596–600. [PubMed: 21251912]

[13]. Funato Y, Hayashi T, Irino Y, Takenawa T, Miki H, Nucleoredoxin regulates glucose metabolism via phosphofructokinase 1, Biochemical and biophysical research communications 440(4) 737–42. [PubMed: 24120946]

[14]. Arellanes-Robledo J, Reyes-Gordillo K, Shah R, Dominguez-Rosales JA, Hernandez-Nazara ZH, Ramirez F, Rojkind M, Lakshman MR, Fibrogenic actions of acetaldehyde are beta-catenin dependent but Wingless independent: a critical role of nucleoredoxin and reactive oxygen species in human hepatic stellate cells, Free radical biology & medicine 65 (2013) 1487–96. [PubMed: 23880292]

[15]. Bertola A, Mathews S, Ki SH, Wang H, Gao B, Mouse model of chronic and binge ethanol feeding (the NIAAA model), Nat Protoc 8(3) (2013) 627–37. [PubMed: 23449255]

[16]. Day CP, James OF, Steatohepatitis: a tale of two “hits”?, Gastroenterology 114(4) (1998) 842–5. [PubMed: 9547102]

[17]. Varatharajalu R, Garige M, Leckey LC, Arellanes-Robledo J, Reyes-Gordillo K, Shah R, Lakshman MR, Adverse signaling of scavenger receptor class B1 and PGC1s in alcoholic hepatosteatosis and steatohepatitis and protection by betaine in rat, The American journal of pathology 184(7) (2014) 2035–44. [PubMed: 24814604]

[18]. Svegliati-Baroni G, Ridolfi F, Di Sario A, Saccomanno S, Bendia E, Benedetti A, Greenwel P, Intracellular signaling pathways involved in acetaldehyde-induced collagen and fibronectin gene expression in human hepatic stellate cells, Hepatology (Baltimore, Md 33(5) (2001) 1130–40.

[19]. Donohue TM, Osna NA, Clemens DL, Recombinant Hep G2 cells that express alcohol dehydrogenase and cytochrome P450 2E1 as a model of ethanol-elicited cytotoxicity, The international journal of biochemistry & cell biology 38(1) (2006) 92–101. [PubMed: 16181800]

[20]. Geerts A, History, heterogeneity, developmental biology, and functions of quiescent hepatic stellate cells, Seminars in liver disease 21(3) (2001) 311–35. [PubMed: 11586463]

[21]. Qin Y, Li L, Pan W, Wu D, Regulation of phosphatidylinositol kinases and metabolism by Wnt3a and Dvl, The Journal of biological chemistry 284(34) (2009) 22544–8. [PubMed: 19561074]

[22]. Irie F, Okuno M, Pasquale EB, Yamaguchi Y, EphrinB-EphB signalling regulates clathrin-mediated endocytosis through tyrosine phosphorylation of synaptojanin 1, Nature cell biology 7(5) (2005) 501–9. [PubMed: 15821731]

[23]. Livak KJ, Schmittgen TD, Analysis of relative gene expression data using realtime quantitative PCR and the 2(-Delta Delta C(T)) Method, Methods (San Diego, Calif 25(4) (2001) 402–8.

[24]. Lei N, Franken L, Ruzehaji N, Offenhauser C, Cowin AJ, Murray RZ, Flightless, secreted through a late endosome/lysosome pathway, binds LPS and dampens cytokine secretion, Journal of cell science 125(Pt 18) 4288–96. [PubMed: 22718342]

[25]. Akerboom TP, Sies H, Assay of glutathione, glutathione disulfide, and glutathione mixed disulfides in biological samples, Methods in enzymology 77 (1981) 373–82. [PubMed: 7329314]

[26]. Rogstad SM, Sorkina T, Sorkin A, Wu CC, Improved precision of proteomic measurements in immunoprecipitation based purifications using relative quantitation, Anal Chem 85(9) (2013) 4301–6. [PubMed: 23517085]

[27]. Gao C, Chen YG, Dishevelled: The hub of Wnt signaling, Cellular signalling 22(5) 717–27. [PubMed: 20006983]

[28]. Kawai S, Enzan H, Hayashi Y, Jin YL, Guo LM, Miyazaki E, Toi M, Kuroda N, Hiroi M, Saibara T, Nakayama H, Vinculin: a novel marker for quiescent and activated hepatic stellate cells in human and rat livers, Virchows Arch 443(1) (2003) 78–86. [PubMed: 12719976]

[29]. Zhu H, Jia Z, Misra H, Li YR, Oxidative stress and redox signaling mechanisms of alcoholic liver disease: updated experimental and clinical evidence, Journal of digestive diseases 13(3) (2012) 133–42. [PubMed: 22356308]

[30]. Kurooka H, Kato K, Minoguchi S, Takahashi Y, Ikeda J, Habu S, Osawa N, Buchberg AM, Moriwaki K, Shisa H, Honjo T, Cloning and characterization of the nucleoredoxin gene that encodes a novel nuclear protein related to thioredoxin, Genomics 39(3) (1997) 331–9. [PubMed: 9119370]

[31]. Lee YN, Gao Y, Wang HY, Differential mediation of the Wnt canonical pathway by mammalian Dishevelleds-1, −2, and −3, Cellular signalling 20(2) (2008) 443–52. [PubMed: 18093802]

[32]. Liu LJ, Xie SX, Chen YT, Xue JL, Zhang CJ, Zhu F, Aberrant regulation of Wnt signaling in hepatocellular carcinoma, World J Gastroenterol 22(33) (2016) 748699.

[33]. Sethi JK, Vidal-Puig A, Wnt signalling and the control of cellular metabolism, The Biochemical journal 427(1) (2010) 1–17. [PubMed: 20226003]

[34]. Pan W, Choi SC, Wang H, Qin Y, Volpicelli-Daley L, Swan L, Lucast L, Khoo C, Zhang X, Li L, Abrams CS, Sokol SY, Wu D, Wnt3a-mediated formation of phosphatidylinositol 4,5-bisphosphate regulates LRP6 phosphorylation, Science (New York, N.Y 321(5894) (2008) 1350–3.

[35]. Rao RK, Seth A, Sheth P, Recent Advances in Alcoholic Liver Disease I. Role of intestinal permeability and endotoxemia in alcoholic liver disease, American journal of physiology 286(6) (2004) G881–4. [PubMed: 15132946]

[36]. Seki E, Brenner DA, Toll-like receptors and adaptor molecules in liver disease: update, Hepatology (Baltimore, Md 48(1) (2008) 322–35.

[37]. Crispe IN, Giannandrea M, Klein I, John B, Sampson B, Wuensch S, Cellular and molecular mechanisms of liver tolerance, Immunological reviews 213 (2006) 10118.

[38]. Li X, Wang Z, Zou Y, Lu E, Duan J, Yang H, Wu Q, Zhao X, Wang Y, You L, He L, Xi T, Yang Y, Pretreatment with lipopolysaccharide attenuates diethylnitrosamine-caused liver injury in mice via TLR4-dependent induction of Kupffer cell M2 polarization, Immunol Res 62(2) (2015) 137–45. [PubMed: 25846584]

[39]. Yu LX, Yan HX, Liu Q, Yang W, Wu HP, Dong W, Tang L, Lin Y, He YQ, Zou SS, Wang C, Zhang HL, Cao GW, Wu MC, Wang HY, Endotoxin accumulation prevents carcinogen-induced apoptosis and promotes liver tumorigenesis in rodents, Hepatology (Baltimore, Md 52(4) (2010) 1322–33.

[40]. Dai Q, Pruett SB, Ethanol suppresses LPS-induced Toll-like receptor 4 clustering, reorganization of the actin cytoskeleton, and associated TNF-alpha production, Alcoholism, clinical and experimental research 30(8) (2006) 1436–44.

[41]. Balla T, Phosphoinositides: tiny lipids with giant impact on cell regulation, Physiol Rev 93(3) (2013) 1019–137. [PubMed: 23899561]

[42]. Di Paolo G, De Camilli P, Phosphoinositides in cell regulation and membrane dynamics, Nature 443(7112) (2006) 651–7. [PubMed: 17035995]

[43]. Peyrou M, Bourgoin L, Foti M, PTEN in liver diseases and cancer, World J Gastroenterol 16(37) (2010) 4627–33. [PubMed: 20872961]

[44]. Trotard M, Lepere-Douard C, Regeard M, Piquet-Pellorce C, Lavillette D, Cosset FL, Gripon P, Le Seyec J, Kinases required in hepatitis C virus entry and replication highlighted by small interference RNA screening, FASEB J 23(11) (2009) 3780–9. [PubMed: 19608626]

[45]. Cohen JI, Nagy LE, Pathogenesis of alcoholic liver disease: interactions between parenchymal and non-parenchymal cells, Journal of digestive diseases 12(1) 3–9. [PubMed: 21091930]

[46]. Lieber CS, ALCOHOL: its metabolism and interaction with nutrients, Annual review of nutrition 20 (2000) 395–430.

[47]. Casini A, Pellegrini G, Ceni E, Salzano R, Parola M, Robino G, Milani S, Dianzani MU, Surrenti C, Human hepatic stellate cells express class I alcohol dehydrogenase and aldehyde dehydrogenase but not cytochrome P4502E1, Journal of hepatology 28(1) (1998) 40–5. [PubMed: 9537862]

[48]. Rojkind M, Reyes-Gordillo K, Hepatic Stellate Cells, in: Arias I (Ed.), The Liver, Biology and Pathobiology, John Wiley & Sons, Oxford, 2009, pp. 407–432.

[49]. Nieto N, Oxidative-stress and IL-6 mediate the fibrogenic effects of [corrected] Kupffer cells on stellate cells, Hepatology (Baltimore, Md 44(6) (2006) 1487–501.

[50]. Wirz W, Antoine M, Tag CG, Gressner AM, Korff T, Hellerbrand C, Kiefer P, Hepatic stellate cells display a functional vascular smooth muscle cell phenotype in a three-dimensional co-culture model with endothelial cells, Differentiation 76(7) (2008) 784–94. [PubMed: 18177423]

[51]. Giraudi PJ, Becerra VJ, Marin V, Chavez-Tapia NC, Tiribelli C, Rosso N, The importance of the interaction between hepatocyte and hepatic stellate cells in fibrogenesis induced by fatty accumulation, Experimental and molecular pathology 98(1) (2015) 85–92. [PubMed: 25533546]

[52]. Yang X, Wang X, Huang X, Hang R, Zhang X, Tang B, A hybrid co-culture model with endothelial cells designed for the hepatic tissue engineering, J Mater Sci Mater Med 28(9) (2017) 139. [PubMed: 28812179]

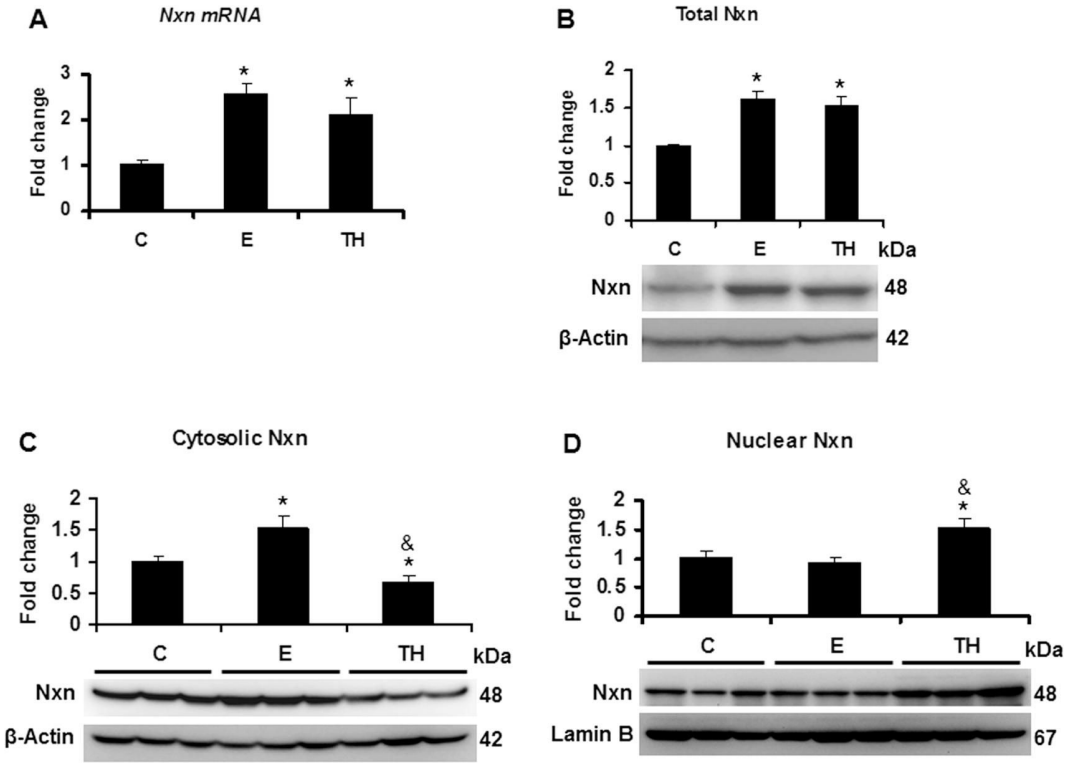

Fig. 1. Effect of ethanol and LPS on Nxn status in the mice liver.

Total, cytosolic and nuclear protein, and total RNA extracted from livers of female wild-type C57BL/6 mice were used for western blot and qPCR analyses, respectively. (**A**) *Nxn* mRNA expression and (**B**) total protein levels of Nxn. (**C**) Cytosolic and (**D**) nuclear Nxn compartmentalized levels. mRNA expression was normalized to *18s mRNA* and cytosolic and nuclear protein levels were normalized to β-actin and Lamin B levels, respectively; these were used as house-keeping controls. Values are expressed as fold change compared to controls. Bars represent the mean ± SE. Statistically different from *****C and from **&**E groups, $p<.05$. **C**, Control; **E**, Ethanol/Binge; **TH**, Ethanol/Binge/LPS model.

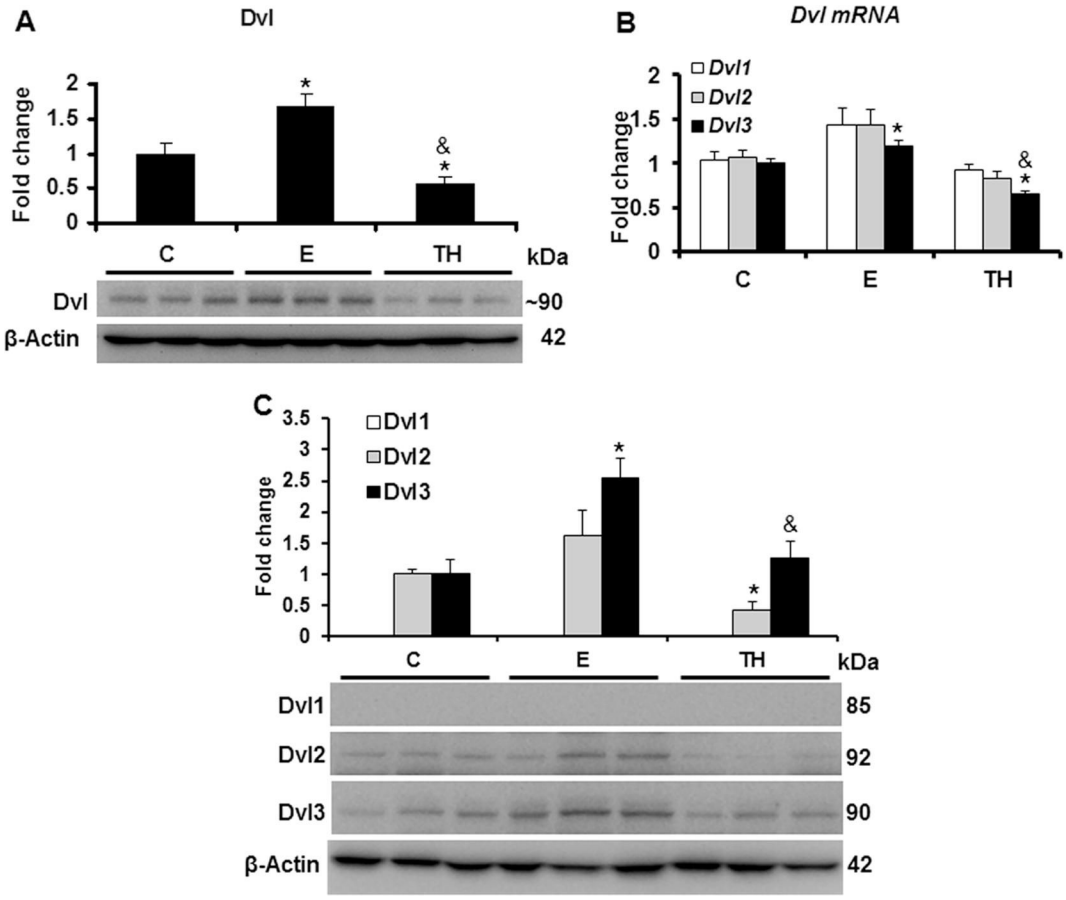

Fig. 2. Effect of ethanol and LPS on Dvl status in the mice liver.

Total protein and RNA extracted from mice livers were used for western blot and qPCR analyses, respectively. (**A**) Total Dvl protein levels. This band was detected by using and anti-Dvl antibody that recognizes all the Dvl (Dvl1–3) variants (for details see Materials and methods). (**B**) Expression of *Dvl* variant genes; (**C**) Protein levels of Dvl1, Dvl2 and Dvl3 variants. While mRNA expression was normalized to *18s* mRNA, Dvl, Dvl1, Dvl2 and Dvl3 protein levels were normalized to β-actin; these were used as house-keeping controls. Values are expressed as fold change compared to controls. Bars represent the mean ± SE. Statistically different from *****C and from **&**E groups, $p<.05$. **C**, Control; **E**, Ethanol/Binge; **TH**, Ethanol/Binge/LPS model.

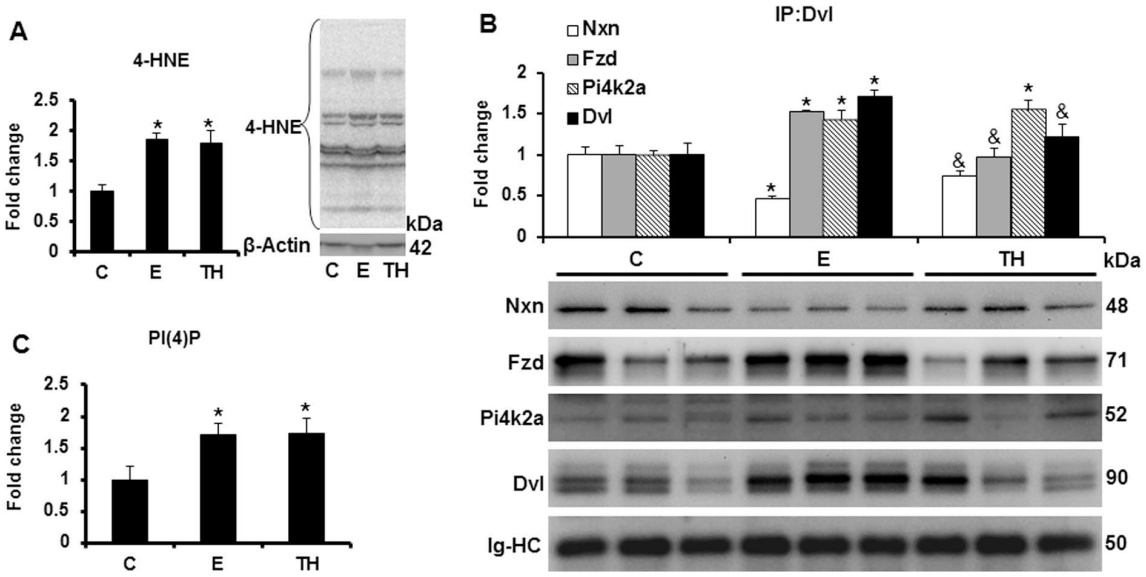

Fig. 3. Effect of ethanol and LPS on Nxn/Dvl interaction and PI(4)P production *in vivo*.

Total protein extracts from mice livers were used for immnumoprecipitation and western blot analyses, and total lipid extracts were used for PI(4)P quantification by ELISA. (**A**) 4-HNE adduct levels; (**B**) Immunoprecipitation of Dvl coprecipitated Nxn, Fzd and Pi4k2a proteins. Dvl bands were detected by using and anti-Dvl antibody that recognizes all the Dvl (Dvl1–3) variants (for details see Materials and methods). (**C**) Quantification of PI(4)P levels. While β-actin expression was used to normalize 4-HNE adduct levels, that of the immunoglobulin heavy chain used for immunoprecipitation was used to normalize the immunoprecipitated. Values are expressed as fold change compared to controls. Bars represent the mean ± SE. Statistically different from *****C and from **&**E groups, $p<.05$. **C**, Control; **E**, Ethanol/Binger; **TH**, Ethanol/Binge/LPS model; **IgHC**, Immunoglobulin heavy chain.

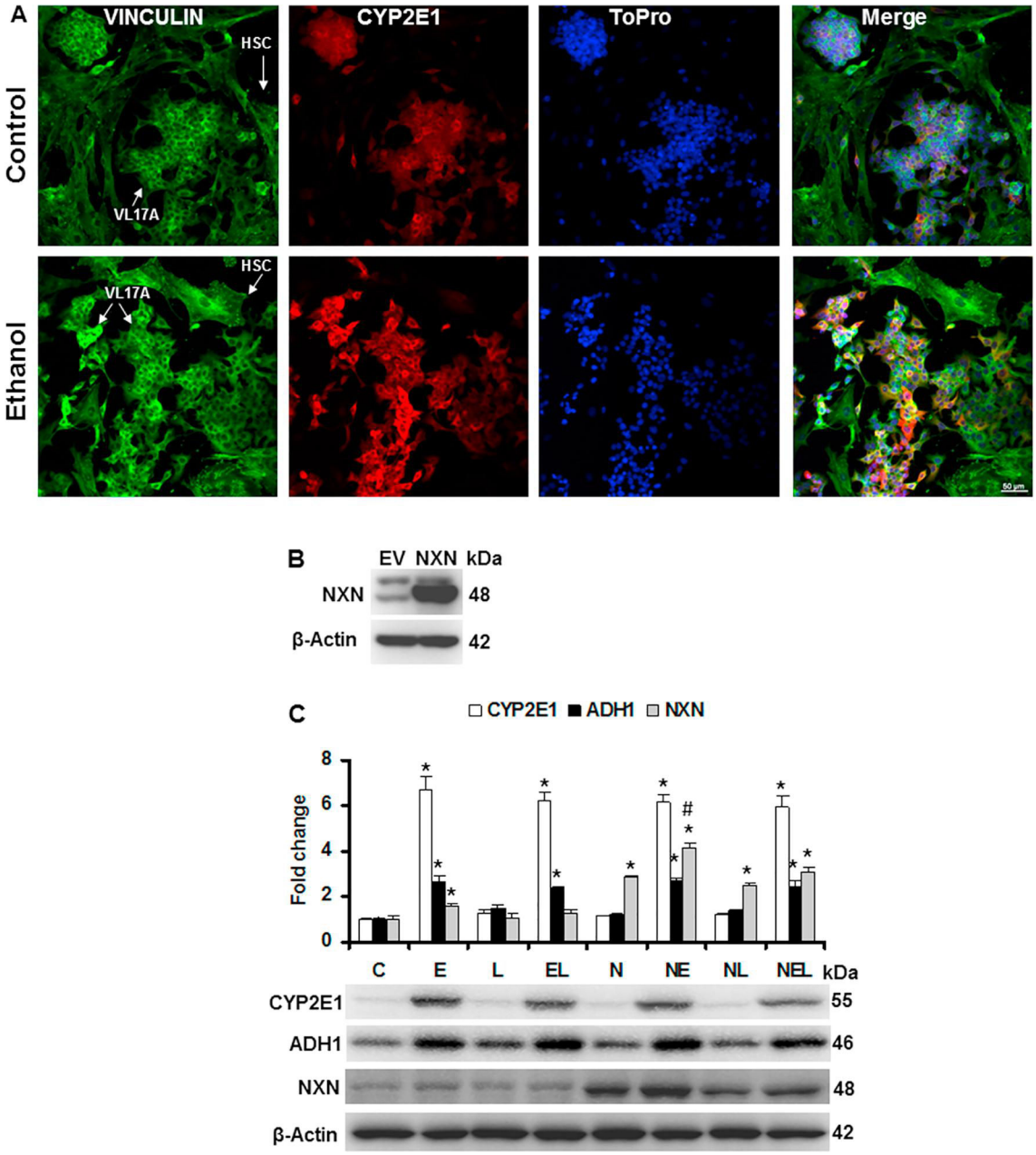

Fig. 4. Ethanol and LPS effects on CYP2E1, ADH1 and NXN expression levels in the HSC/VL17A co-culture system.

For immunofluorescence, co-cultures were plated in two-well chamber slides and then cells were exposed to 100 mM ethanol for 48 h. (**A**) Analysis was performed in 4% formaldehyde fixed cells with mouse anti-Vinculin and rabbit anti-CYP2E1 antibodies and nuclei were staining with ToPro. Arrows show HSC and VL17A cells. (**B**) Efficiency of NXN transfection. Co-cultures were transfected either with 1 μg/ml of empty vector (EV) or NXN expressing vector and total protein was extracted after 48 h. (**C**) Co-cultures were exposed to 100 mM ethanol for 48 h and then LPS (1 μg/ml) was added and incubated for 3 h. Total protein was extracted and CYP2E1, ADH1 and NXN levels were determined by western blot. Protein levels were normalized to β-actin; this was used as house-keeping control.

Three independent experiments were carried out in duplicated. Values are expressed as fold change compared to controls. Bars represent the mean ± SE. Statistically different from *****C and $^{\#}$N groups, $p<.05$. **C**, Control; **E**, Ethanol; **L**, LPS; **EL**, Ethanol plus LPS. These groups were transfected with EV which were called untransfected cells. **N**, NXN-transfected cells; these cells were also exposed to **E**, **L** and **EL** treatments; **NE**, **NL** and **NEL**, respectively.

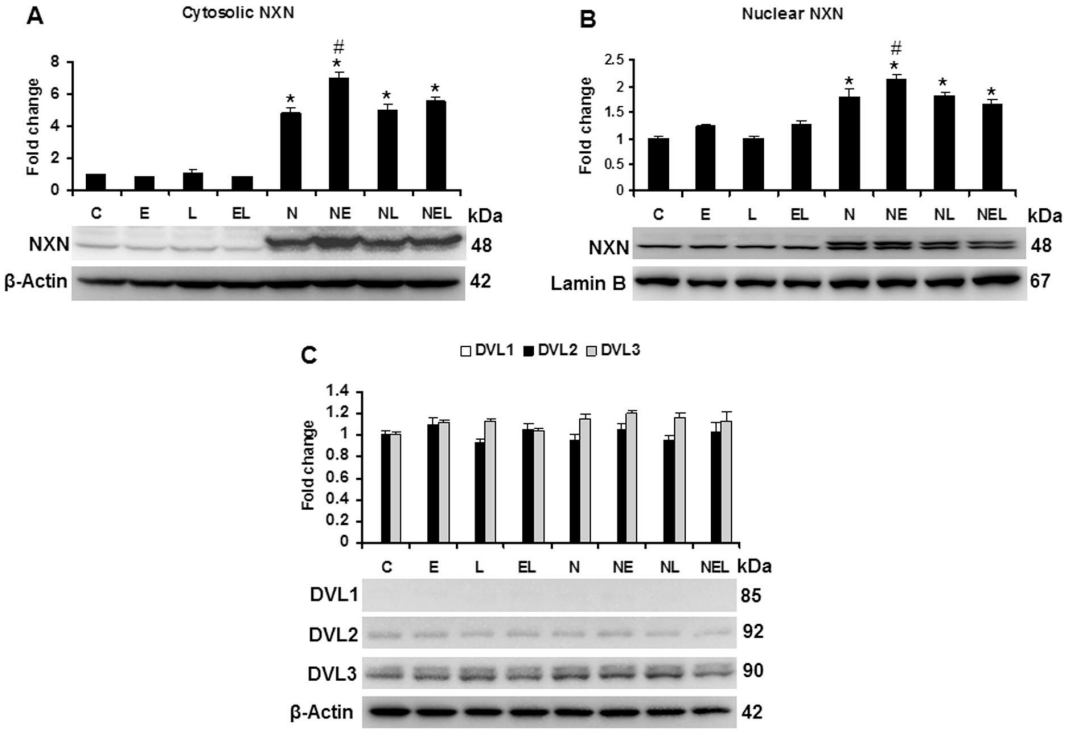

Fig. 5. Ethanol and LPS effects on cytosolic and nuclear NXN, and DVL variants expression levels in the HSC/VL17A co-culture system.

Total, cytosolic and nuclear proteins extracted from co-cultures transfected either with EV or NXN expressing vector and exposed to ethanol and/or LPS were used for western blot analyses. While total and cytosolic protein levels were normalized to β-actin that of nuclear protein was normalized to Lamin B expression levels; these were used as house-keeping controls. Three independent experiments were carried out in duplicated. Values are expressed as fold change compared to controls. Bars represent the mean ± SE. Statistically different from ***C** and #N groups, $p<.05$. **C**, Control; **E**, Ethanol; **L**, LPS; **EL**, Ethanol plus LPS. These groups were transfected with EV which were called untransfected cells. **N**, NXNtransfected cells; these cells were also exposed to **E**, **L** and **EL** treatments; **NE**, **NL** and **NEL**, respectively.

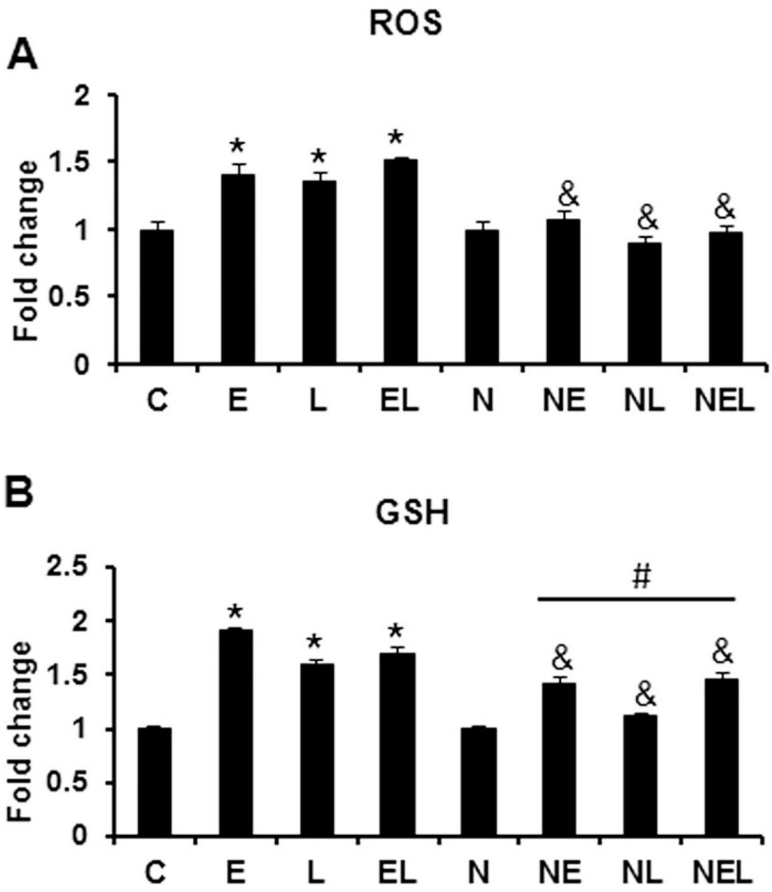

Fig. 6. Ethanol and LPS effects on ROS and GSH levels in the HSC/VL17A coculture system.

Co-cultures transfected either with EV or NXN expressing vector and exposed to ethanol and/or LPS were used for ROS and GSH determinations. (**A**) ROS levels were determined spectrofluometrically in black 96-well microplates by labeling 7×10^3 cells/well approximately with DCFDA. (B) For GSH determination, after different treatments co-cultures were solubilized in 5% 5-sulfosalicylic acid as described in Methods. Three independent experiments were carried out in duplicated. Values are expressed as fold change compared to controls. Bars represent the mean ± SE. Statistically different from *****C, from $^{\#}$N and from $^{\&}$the same treatment in untransfected cells groups, $p<.05$. **C**, Control; **E**, Ethanol; **L**, LPS; **EL**, Ethanol plus LPS. These groups were transfected with EV which were called untransfected cells. **N**, NXN-transfected cells; these cells were also exposed to **E**, **L** and **EL** treatments; **NE**, **NL** and **NEL**, respectively.

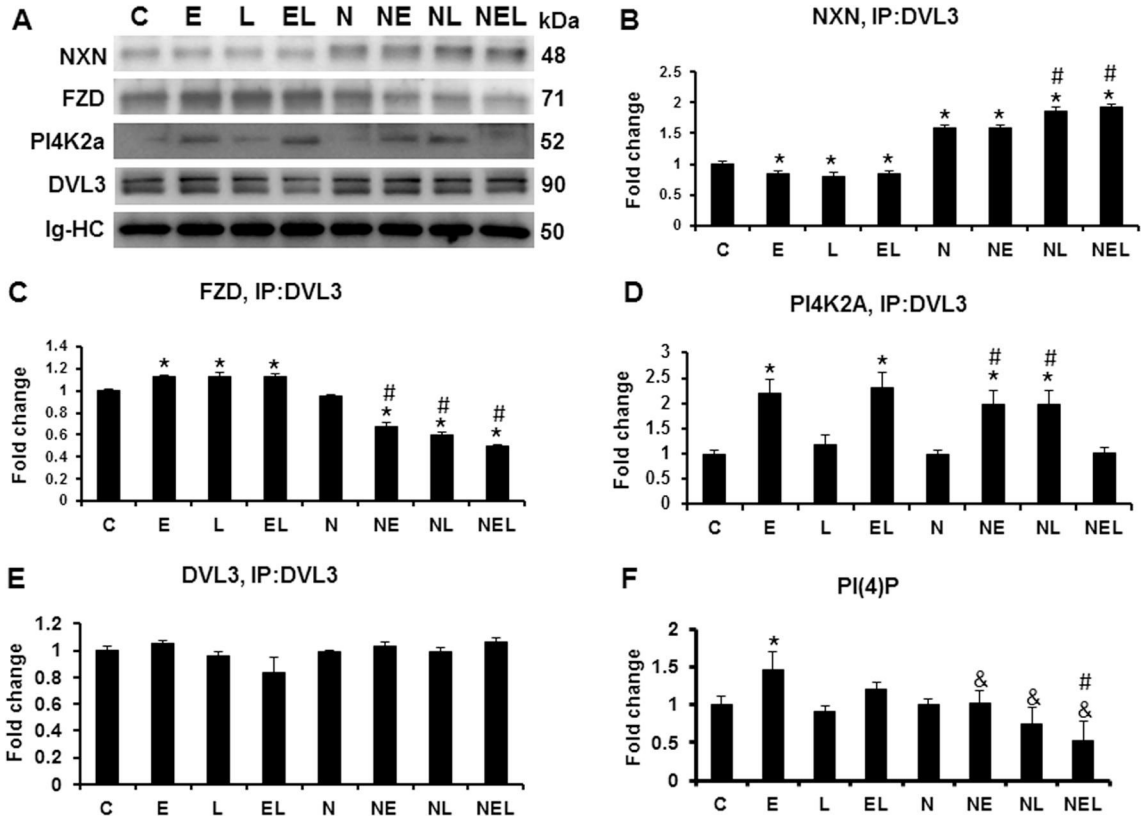

Fig. 7. Ethanol and LPS effect on Nxn/Dvl interaction and PI(4)P production *in vitro*.

Total protein extracts from co-cultures transfected either with EV or NXN expressing vector and exposed to ethanol and/or LPS were used for DVL3 immunoprecipitation analyses. (**A**) Western blot analyses of NXN, FZD and PI4K2A coprecipitated from DVL3 immunoprecipitation. Densitometric quantification of (**B**) NXN, (**C**) FZD and (**D**) PI4K2a co-precipitated, and (**E**) DVL3 precipitated; (**F**) Quantification of PI(4)P levels by ELISA. Co- and immunoprecipitated were normalized to the heavy chain of the immunoglobulin used for immunoprecipitation. Two independent experiments were carried out in duplicated. Values are expressed as fold change compared to controls. Bars represent the mean ± SE. Statistically different from *****C, from **#**N and from **&**the same treatment in untransfected cells groups, $p<.05$. **C**, Control; **E**, Ethanol; **L**, LPS; **EL**, Ethanol plus LPS. These groups were transfected with EV which were called untransfected cells. **N**, NXN-transfected cells; these cells were also exposed to **E**, **L** and **EL** treatments; **NE**, **NL** and **NEL**, respectively. **Ig-HC**, Immunoglobulin heavy chain.

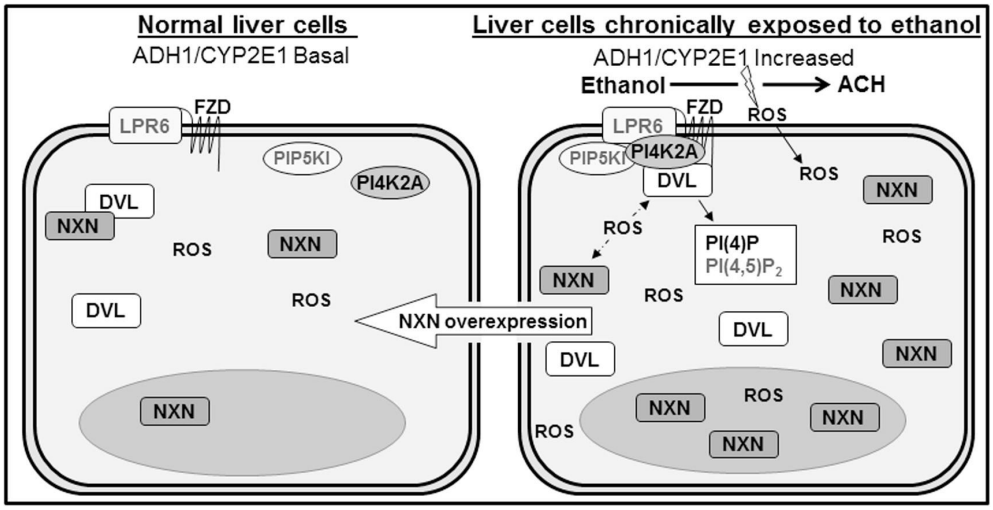

Fig. 8. Model of ethanol effect on NXN/DVL and FZD/DVL/PI4K interactions, PI(4)P production, and their regulation by NXN overexpression.

It is well-known that ethanol metabolism by liver cells mainly produces acetaldehyde (ACH) and ROS, among others sub-products. Our proposed model strongly suggests that elevated ROS levels disrupt NXN/DVL redox sensitive interaction allowing FZD/DVL/PI4K complex formation and binding into LPR6 transmembrane receptor. The formation of this complex in turn stimulates PI(4)P production. Chronic ethanol exposure also increases NXN and DVL protein levels and, preferentially by *in vivo* Ethanol/Binge model effect, NXN is translocated into the nucleus. These events are negligible in control liver cells because the endogenous antioxidant defense systems effectively neutralize oxidative stress thus maintaining the normal homeostatic functioning of NXN. Transfection of NXN expressing vector revels that the molecular alterations induced by ethanol exposure might be partially reverted by the overexpression of NXN in the co-culture system. Dotted arrows indicate the disruption of NXN/DVL interaction by high ROS levels. Molecules indicated in grey were not evaluated.